THE JOURNAL OF BIOLOGICAL CHEMISTRY Vol. 279, No. 35, Issue of August 27, pp. 36504–36515, 2004

Printed in U.S.A.

Imbalanced Base Excision Repair in Response to Folate Deficiency Is Accelerated by Polymerase β Haploinsufficiency*

Received for publication, May 10, 2004, and in revised form, June 18, 2004
Published, JBC Papers in Press, June 24, 2004, DOI 10.1074/jbc.M405185200

Diane C. Cabelof‡, Julian J. Raffoul‡, Jun Nakamura§, Diksha Kapoor‡, Hala Abdalla‡, and Ahmad R. Heydari‡¶

From the ‡Department of Nutrition and Food Science, Wayne State University, Detroit, Michigan 48202 and the §Department of Environmental Sciences and Engineering, University of North Carolina, Chapel Hill, North Carolina 27599

The mechanism by which folate deficiency influences carcinogenesis is not well established, but a phenotype of DNA strand breaks, mutations, and chromosomal instability suggests an inability to repair DNA damage. To elucidate the mechanism by which folate deficiency influences carcinogenicity, we have analyzed the effect of folate deficiency on base excision repair (BER), the pathway responsible for repairing uracil in DNA. We observe an up-regulation in initiation of BER in liver of the folate-deficient mice, as evidenced by an increase in uracil DNA glycosylase protein (30%, $p < 0.01$) and activity (31%, $p < 0.05$). However, no up-regulation in either BER or its rate-determining enzyme, DNA polymerase β (β-pol) is observed in response to folate deficiency. Accordingly, an accumulation of repair intermediates in the form of DNA single strand breaks (37% increase, $p < 0.03$) is observed. These data indicate that folate deficiency alters the balance and coordination of BER by stimulating initiation without subsequently stimulating the completion of repair, resulting in a functional BER deficiency. In directly establishing that the inability to induce β-pol and mount a BER response when folate is deficient is causative in the accumulation of toxic repair intermediates, β-pol-haploinsufficient mice subjected to folate deficiency displayed additional increases in DNA single strand breaks (52% increase, $p < 0.05$) as well as accumulation in aldehydic DNA lesions (38% increase, $p < 0.01$). Since young β-pol-haploinsufficient mice do not spontaneously exhibit increased levels of these repair intermediates, these data demonstrate that folate deficiency and β-pol haploinsufficiency interact to increase the accumulation of DNA damage. In addition to establishing a direct role for β-pol in the phenotype expressed by folate deficiency, these data are also consistent with the concept that repair of uracil and abasic sites is more efficient than repair of oxidized bases.

In human studies, folate deficiency is associated with cancers of the lung, cervix, brain, esophagus, pancreas, breast, colon, and liver (reviewed in Refs. 1 and 2). In support of the epidemiology, the role of folate in the development of both colon and liver cancer has been experimentally demonstrated in animal studies. Folate deficiency enhances the carcinogenic effect of dimethylhydrazine (3), whereas folate supplementation is protective (4). Folate/methyl deficiency results in hepatocarcinogenesis (5). Additionally, livers of folate/methyl-deficient rats accumulate preneoplastic changes in response to folate deficiency (6). It is suggested that the carcinogenic properties of folate deficiency are related to a reduction in *S*-adenosylmethionine levels altering DNA methylation status and/or to depletion of thymidylate resulting in increased uracil content of DNA. Additionally, folate is required for *de novo* purine biosynthesis. Which of these factors may be responsible for inducing carcinogenesis is presently unknown.

Whereas the underlying mechanism connecting folate deficiency to cancer remains unknown, it is clear that folate deficiency induces a phenotype suggestive of an inability to repair DNA damage. The accumulation of strand breaks, mutations, and chromosomal instability observed in response to folate deficiency all suggest that DNA repair capacity is inhibited. In support of this, folate-deficient cells and animals inefficiently repair alkylation damage (7). Folate deficiency acts synergistically with ethane methyl sulfonate in Chinese hamster ovary cells (8), suggesting an inability to repair ethane methyl sulfonate-induced damage. Folate depletion in human lymphocytes sensitizes to oxidative damage induced by hydrogen peroxide (9). Human colon epithelial cells grown in folate-deficient medium are unable to repair damages induced by methylmethane sulfonate and hydrogen peroxide (10). Folate deficiency impairs the ability of neurons and colonocytes to repair DNA damage (11, 12). These data suggest that the pathway responsible for repairing these damages may be ineffective when folate is limiting by demonstrating a persistence of DNA damage but stop short of directly measuring DNA repair capacity. The objectives of this study are to directly measure the effects of folate deficiency on DNA repair capacity and to begin identifying the molecular mechanisms responsible for precipitating a phenotype of cancer susceptibility when folate is deficient.

Uracil has been shown to accumulate in response to folate deficiency (9, 10, 13–15). The DNA repair pathway for removal of uracil is the base excision repair (BER)[1] pathway. The BER pathway repairs small, non-helix-distorting lesions in the DNA. In the process of repairing uracil, the following sequence of events occurs. Uracil-DNA glycosylase (UDG), a monofunc-

* This work was supported by National Institutes of Health Grant 1R21-DK62256 (to A. R. H.) and a grant from the American Institute for Cancer Research (to A. R. H.). The costs of publication of this article were defrayed in part by the payment of page charges. This article must therefore be hereby marked "*advertisement*" in accordance with 18 U.S.C. Section 1734 solely to indicate this fact.

¶ To whom correspondence and reprint requests should be addressed: Dept. of Nutrition & Food Science, 3009 Science Hall, Wayne State University, Detroit, MI 48202. Tel.: 313-577-2753; Fax: 313-577-8616; E-mail: ahmad.heydari@wayne.edu.

[1] The abbreviations used are: BER, base excision repair; UDG, uracil-DNA glycosylase; Ape, AP endonuclease; β-pol, polymerase β; ASB, aldehyde-reactive probe slot blot; ADL, aldehydic DNA lesion; DTT, dithiothreitol; I.D.V., integrated density value; ROPS, random oligonucleotide-primed synthesis; TEMPO, 2,2,6,6-tetramethylpiperidin-oxyl.

tional glycosylase, excises uracil from the DNA backbone, creating a transient abasic site. AP endonuclease 1 (Ape1) cleaves the DNA backbone to allow for incorporation of a correct nucleotide by DNA polymerase β (β-pol). This step results in the transient formation of both a 3′-OH-containing DNA single strand break and a deoxyribose phosphate flap containing an aldehydic group. β-pol also performs the rate-limiting step of deoxyribose flap excision (16), at which point only the 3′-OH group remains until ligation occurs (ligase 1 or ligase 3-XRCC1 complex), at which point the strand break is fully resolved. Typically, BER functions as a tightly coordinated sequence of enzymatic events such that damage is removed, repair is completed, and intermediate products generated during repair do not accumulate. Mice with gene-targeted disruptions in the rate-limiting step of BER exhibit a dysregulation in this coordination and accumulate DNA single strand breaks both spontaneously and in response to carcinogen exposure, have a reduced DNA damage threshold, and exhibit genomic instability in the forms of both mutation induction and chromosomal damage (17). The phenotype of folate deficiency includes accumulation of strand breaks (9, 10, 15, 18, 19), reduced tolerance to DNA-damaging agents, increased mutation induction (7, 8, 20), and chromosomal instability (21, 22) (*i.e.* folate deficiency induces a phenotype identical to BER deficiency).

The objective of this study was to directly determine the effect of folate deficiency on base excision repair capacity. Because BER is DNA damage-inducible (23, 24), we expected to observe an induction in the activity of this repair pathway in response to the DNA damage induced by folate deficiency. However, in response to folate deficiency we fail to observe an up-regulation in either BER or the rate-determining enzyme in the pathway, β-pol. This lack of response by the BER pathway should result in an accumulation of the DNA damage induced by folate deficiency. We provide evidence that the initial step of BER, glycosylase-initiated removal of uracil, is up-regulated in response to folate deficiency, without a coordinating increase in activity of the subsequent steps of repair. This dysregulation of BER induces a state of BER deficiency mimicking that observed in mice heterozygous for β-pol. Our data demonstrate that in response to folate deficiency repair is initiated but not completed, resulting in an accumulation of DNA repair intermediate products that are genotoxic (25). Since BER deficiency increases cancer susceptibility, this functional BER deficiency in response to folate deficiency may provide an important mechanistic explanation for the increased cancer risk associated with folate deficiency. As such, human polymorphisms and functional mutations within the β-pol gene may interact with folate deficiency to increase cancer risk. This hypothesis is supported by our data demonstrating that folate deficiency results in a greater accumulation of DNA damage in mice haploinsufficient for β-pol.

EXPERIMENTAL PROCEDURES

Animals

Experiments were performed in young (3–4 months) male C57BL/6-specific pathogen-free mice in accordance with the National Institutes of Health guidelines for the use and care of laboratory animals. The Wayne State University Animal Investigation Committee approved the animal protocol. Mice were maintained on a 12-h light/dark cycle and fed standard mouse chow and water *ad libitum*. Mice heterozygous for the DNA polymerase β gene (β-pol$^{+/-}$) were created in Rajewsky's laboratory by deletion of the promoter and the first exon of the β-pol gene (26). The animals appear to be normal and are fertile; there is no retardation in food intake, weight gain, or growth rate. The genotype of the mice was determined as described previously (17).

At 3–4 months of age, 20 β-pol$^{+/+}$ and 20 β-pol$^{+/-}$ mice were randomly assigned to two dietary groups and were fed AIN93G-purified isoenergetic diets. (Dyets, Inc., Lehigh Valley, PA). The control group received a folate adequate diet containing 2 mg/kg folic acid. The experimental group received a folate-deficient diet containing 0 mg/kg folic acid. Diets were stored at −20 °C. 1% succinyl sulfathiazole was added to all diets. The animals' food intake and body weights were monitored twice weekly to monitor for signs of toxicity (*i.e.* weight loss), and the experimental diets were continued for 8 weeks. Animals were anesthetized under CO_2 and sacrificed by cervical dislocation. Whole blood was collected, and tissues were flash frozen and stored in liquid nitrogen.

Folate Assay

Serum folate levels were measured using the SimulTRAC-SNB radioassay kit for vitamin B_{12} (^{57}Co) and folate (^{125}I) per the manufacturer's protocol (ICN Diagnostics, Orangeburg, NY). Blood was collected at time of sacrifice and allowed to clot at room temperature for 60 min. Samples were centrifuged, and serum was collected for immediate analysis of serum folate levels. Standards provided in the kit were used to generate a standard curve for determination of sample folate values. Radioactivity was measured by a γ-counter, and values were calculated as described by the manufacturer for both serum folate and serum B_{12}.

Isolation of DNA

TEMPO Extraction of DNA—Liver DNA for the aldehyde-reactive probe slot blot (ASB) assay was extracted according to the method described by Hofer and Moller (27) with some modifications. This method minimizes artifactual DNA damage by using 20 mM TEMPO in all solutions and reagents and by minimizing heat treatment of DNA. Briefly, 100 mg of liver tissue was homogenized in 5 ml of ice-cold phosphate-buffered saline with 20 mM TEMPO and centrifuged at 2000 × *g* at 4 °C for 5 min. Supernatant was decanted, and pellet was resuspended in 2.5 ml of lysis buffer (pH 8.0; Applied Biosystems, Foster City, CA) with 20 mM TEMPO. Proteinase K (30 units; Ambion, Austin, TX) was added, and samples were incubated overnight at 4 °C. DNA was extracted with 2.5 ml 70% phenol/water/chloroform (Applied Biosystems, Foster City, CA) with 20 mM TEMPO. Further extraction with 2.5 ml of sevag (chloroform/isoamyl alcohol, 24:1) with 20 mM TEMPO was completed. DNA was precipitated using 7.5% 4 M NaCl and 2 volumes of 100% cold ethanol, and pellet was washed in 70% ethanol. The pellet was resuspended in 700 μl of phosphate-buffered saline with 20 mM TEMPO and rehydrated at 4 °C. The samples were then treated with RNase A (2 μg) and RNase T1 (1,000 units; Ambion, Austin, TX) at 37 °C for 30 min to digest the RNA contamination. DNA was cold ethanol-precipitated and resuspended in 400 μl of deionized water at 4 °C. DNA was stored at −70 °C.

Gravity Tip Column Extraction of DNA—DNA for the random oligonucleotide-primed synthesis (ROPS) assay was isolated using Qiagen (Valencia, CA) gravity tip columns as described in the manufacturer's protocol. This method generates large fragments of DNA (up to 150 kb) while minimizing shearing.

ASB Assay

Detection of aldehydic DNA lesions (ADLs) was carried out by ASB as described previously (28) with slight modifications. DNA (8 μg) was incubated in 30 μl of phosphate-buffered saline with 2 mM aldehyde reactive probe (Dojindo Laboratories, Kumamoto, Japan) at 37 °C for 10 min. DNA was precipitated by the cold ethanol method (described above) and resuspended in 1× TE buffer overnight at 4 °C. DNA was heat-denatured at 100 °C for 10 min, quickly chilled on ice, and mixed with an equal volume of 2 M ammonium acetate. The nitrocellulose membrane (Schleicher & Schuell) was prewet in deionized water and washed for 10 min in 1 mM ammonium acetate. DNA was immobilized on the pretreated nitrocellulose membrane using an Invitrogen filtration manifold system. The membrane was washed in 5× SSC for 15 min at 37 °C and then baked under vacuum at 80 °C for 30 min. The dried membrane was incubated in a hybridization buffer (20 mM Tris, pH 7.5, 0.1 M NaCl, 1 mM EDTA, 0.5% (w/v) casein, 0.25% (w/v) bovine serum albumin, 0.1% (v/v) Tween 20) for 30 min at room temperature. The membrane was then incubated in fresh hybridization buffer containing 100 μl of streptavidin-conjugated horseradish peroxidase (BioGenex, San Ramon, CA) at room temperature for 45 min. Following incubation in horseradish peroxidase, the membrane was washed three times for 5 min each at 37 °C in TBS, pH 7.5 (0.26 M NaCl, 1 mM EDTA, 20 mM Tris, pH 7.5, 0.1% Tween 20). Membrane was incubated in ECL (Pierce) for 5 min at room temperature and visualized using a ChemiImager™ system (AlphaInnotech, San Leandro, CA).

Isolation of Crude Nuclear Extract

Nuclear proteins for Western analyses and enzymatic activity assays were isolated using the Sigma CelLytic™ NuCLEAR™ extraction kit, a

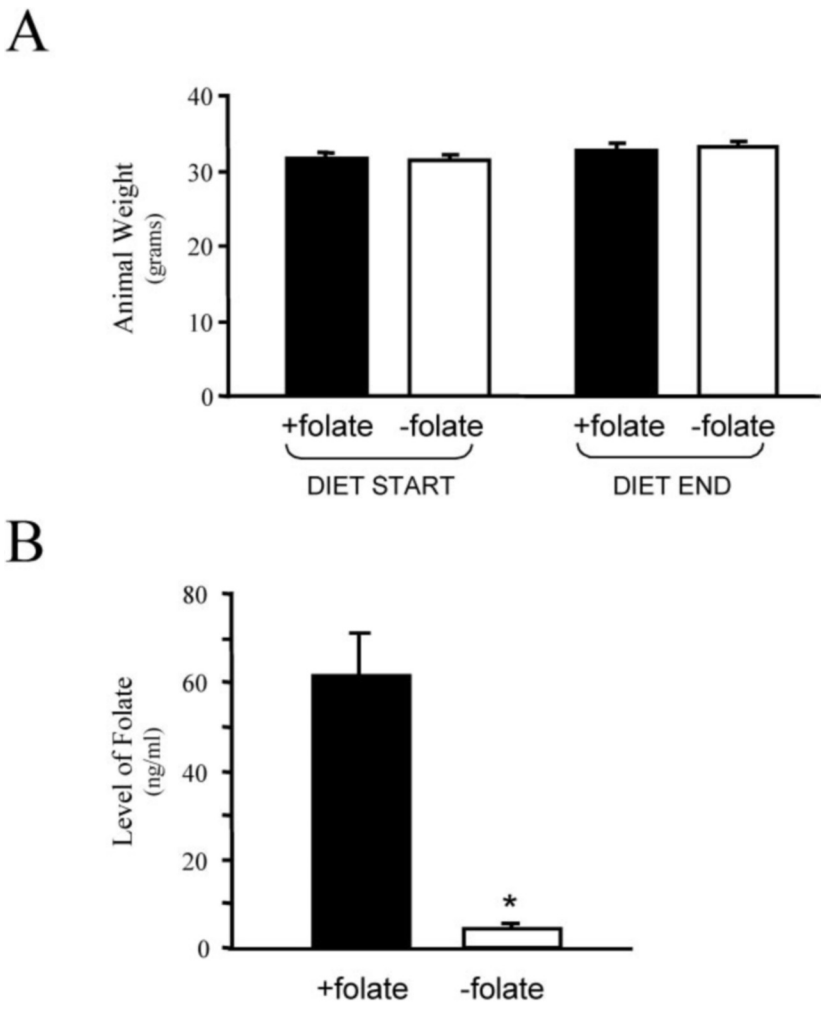

FIG. 1. **Effect of dietary folate on body weight and plasma folate status.** *A*, weight of animals before and after the implementation of the folate-deficient and -adequate diet. Young (3–4 months) male C57BL/6 mice were fed AIN93G purified isoenergetic diets containing either 2 mg/kg folic acid (folate-adequate) or 0 mg/kg folic acid (folate-deficient) as described under "Experimental Procedures." The experimental diets were continued for 8 weeks, and the animals' food intake and body weights were measured twice weekly. The animals' weights in grams are expressed as the means ± S.E. for data obtained from 10 mice in each group. *B*, serum folate levels in mice fed folate-adequate or folate-deficient diets were measured using the SimulTRAC-SNB radioassay kit per the manufacturer's protocol (ICN Diagnostics, Orangeburg, NY). The relative level of folate in plasma is expressed as ng/ml of plasma based on standards provided in the kit, and the data are expressed as the means ± S.E. for data obtained from 10 mice in each group. *Filled bar*, 2 mg/kg folic acid; *open bar*, 0 mg/kg folic acid.

method that disrupts cells with hypotonic buffer, allowing the cytoplasmic fraction to be removed while the nuclear proteins are released from the nuclei by a high salt buffer. All samples and tubes were handled and chilled on ice, and all solutions were made fresh according to the manufacturer's protocol. The extract was snap frozen in liquid nitrogen and stored at −70 °C. In order to remove salt, the crude nuclear extract was dialyzed against 1 liter of dialysis buffer (20 mM Tris-HCl, pH 8.0, 100 mM KCl, 10 mM NaS_2O_5, 0.1 mM DTT, 0.1 mM phenylmethylsulfonyl fluoride, 1 μg/ml pepstatin A) for 4–6 h at 4 °C using Slide-A-Lyzer® mini-dialysis units suspended in a floatation device (Pierce). The dialyzed nuclear extracts were flash frozen in liquid nitrogen and stored at −70 °C. Protein concentrations of the nuclear extracts were determined according to Bradford using Protein Assay Kit I (Bio-Rad).

Western Blot Analyses

Western analysis was performed using liver nuclear extracts (50 μg) subjected to 10% SDS-PAGE and transferred to a Hybond™ ECL™ nitrocellulose membrane (Amersham Biosciences) using a Bio-Rad semidry transfer apparatus. Prior to hybridization, the membranes were stained with MemCode (Pierce) to ensure equal transfer of protein to the membrane. Western blot analysis was accomplished using manufacturer-recommended dilutions of antisera developed against UDG (Santa Cruz Biotechnology, Inc., Santa Cruz, CA), p53 (polyclonal antibody 240; Santa Cruz Biotechnology), β-pol (Ab-1 Clone 18S; NeoMarkers, Fremont, CA), and Ape/Ref1 (Novus Biologicals, Littleton, CO). The bands were detected and quantified using a ChemiImager™ system (AlphaInnotech) after incubation in SuperSignal® West Pico chemiluminescent substrate (Pierce). The data are expressed as the integrated density value (I.D.V.) of the band per μg of protein loaded.

UDG Activity Assay

UDG activity was determined as described by Stuart *et al.* (29). Briefly, the 20-μl reaction contained 70 mM Hepes (pH 7.5), 1 mM EDTA, 1 mM DTT, 75 mM NaCl, 0.5% bovine serum albumin, 90 fmol of 5′-end-labeled single-stranded uracil-containing oligonucleotide that was 3′-protected by an amino-spacer (5′-ATATACCGCGGUCGGC-CGATCAAGCTTATT-3′, MIDLAND, Midland, TX), and 5 μg of liver nuclear extract. Reactions were incubated at 37 °C for 1 h and then terminated by the addition of 5 μg of proteinase K and 1 μl of 10% SDS and incubation at 55 °C for 30 min. DNA was precipitated in glycogen, ammonium acetate, and ethanol at −20 °C overnight, resuspended in a loading buffer containing 80% formamide, 10 mM EDTA, and 1 μg/ml each of bromphenol blue and xylene cyanol FF. Substrate and reaction products were separated on a 20% denaturing sequencing gel. Glycosylase activity (presence of an 11-mer band) was visualized and quantified using a Molecular Imager® System (Bio-Rad) by calculating the relative amount of the 11-mer oligonucleotide product with the unreacted 30-mer substrate (product/product + substrate). The data are expressed as machine counts/μg of protein. Negative controls consisted of the reaction mixture and oligonucleotide in the absence of nuclear extract. 1 unit of uracil DNA glycosylase inhibitor was added to one sample in each reaction to demonstrate that incision activity was the result of UDG specifically and not another uracil-specific glycosylase (*i.e.* SMUG).

Ape Activity Assay

The 5′-endonuclease activity of Ape was analyzed using a quantitative *in vitro* assay that measures the incision of a 26-mer duplex oligonucleotide substrate containing a tetrahydrofuran (F) AP site as previously described (30). A 26-mer oligonucleotide (5′-AATTCACCG-GTACC**F**TCTAGAATTCG-3′) was 5′-end-labeled and annealed to an equimolar amount of the complementary strand (5′-CGAATTCTA-GAGGGTACCGGTGAATT-3′). 2.5 pmol of double strand oligonucleotide was incubated with 100 ng of crude nuclear extract from liver of control and folate-deficient mice for 15 min at 37 °C and stopped by the addition of 50 mM EDTA (reaction mixture; final concentrations: 50 mM Hepes, pH 7.5, 50 mM KCl, 10 mM $MgCl_2$, 2 mM DTT, 1 μg/ml bovine serum albumin, and 0.05% Triton X-100). Reaction products were run

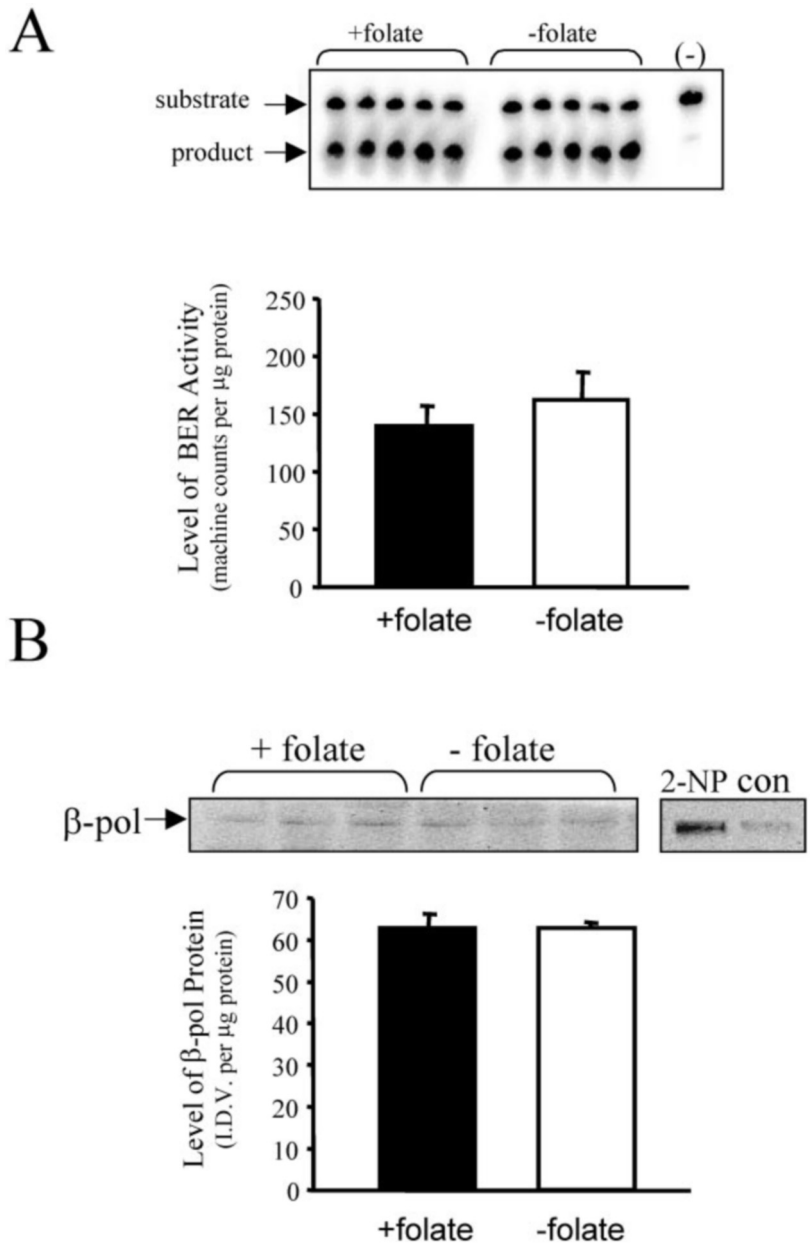

FIG. 2. **Analysis of base excision repair capacity and DNA polymerase β protein in response to folate deficiency in liver.** The experiments were conducted using crude nuclear extracts as described under "Experimental Procedures." *A*, an autoradiograph of a sequencing gel indicating repair activity as visualized by the appearance of a 16-base fragment. The relative level of base excision repair in liver tissue of mice fed the purified isoenergetic diets containing either 2 mg/kg folic acid (folate-adequate) or 0 mg/kg folic acid (folate-deficient) was quantified using a Bio-Rad Molecular Imager® System, and the data were normalized based on the amount of protein used in each reaction. The data are expressed as machine counts/μg of protein. Values represent a mean ± S.E. for data obtained from at least 10 animals in each group. −, G:U mismatch oligonucleotide incubated in the absence of nuclear extract and treated with HpaII restriction endonuclease. *B*, samples of Western blot images of β-pol protein in liver of mice fed the folate-adequate or folate-deficient diets are shown (*left panel*). As a positive control, samples of Western blot for 2-nitropropane-treated mice (*2-NP*; 100 mg/kg body weight) and untreated mice (*con*) are shown (*right panel*). 2-Nitropropane results in up-regulation of β-pol protein level. The relative level of the 39-kDa β-pol protein for samples from mice fed a folate-adequate or folate-deficient diet was determined by Western blot analysis using monoclonal antisera developed against mouse β-pol. The bands were detected and quantified using an AlphaInnotech ChemiImager™ system. The data are expressed as the I.D.V. of the band/μg of protein loaded. Values are expressed as mean ± S.E. for data obtained from at least 10 animals in each group. *Filled bar*, 2 mg/kg folic acid; *open bar*, 0 mg/kg folic acid.

on a 15% denaturing sequencing gel. Endonuclease activity (presence of a 14-mer band) was visualized and quantified using a Molecular Imager® System (Bio-Rad) by calculating the relative amount of the 14-mer oligonucleotide product with the unreacted 26-mer substrate (product/product + substrate). The data are expressed as machine counts/ng of protein.

DNA Base Excision Repair Assay

BER capacity was determined as described previously (17). Briefly, end-labeled and purified 30-bp oligonucleotides (upper strand, 5′-ATATACCGCGGUCGGCCGATCAAGCTTATT-3′; lower strand, 3′-TATATGGCGCCGGCCGGCTAGTTCGAATAA-5′) containing a G:U mismatch and an HpaII restriction site (GGCC) and protected by a 3′ amino spacer were incubated in a reaction mixture (100 mM Tris-HCl, pH 7.5, 5 mM $MgCl_2$, 1 mM DTT, 0.1 mM EDTA, 2 mM ATP, 0.5 mM NAD, 20 μM dNTPs, 5 mM di-Tris-phosphocreatine, 10 units of creatine phosphokinase) with 50 μg of nuclear extract isolated from liver of control and folate-deficient mice. The reaction mixtures were incubated for 30 min at 37 °C, followed by 5 min at 95 °C to stop the reaction. The duplex oligonucleotides were allowed to reanneal for 1 h at room temperature and spun down to pellet the denatured proteins. The duplex oligonucleotides present in the supernatant were treated with 20 units of HpaII (Promega, Madison, WI) for 1 h at 37 °C and separated by electrophoresis on a 20% denaturing sequencing gel. Repair activity (presence of a 16-mer band) is visualized and quantified using a Molecular Imager® System (Bio-Rad) by calculating the ratio of the 16-mer oligonucleotide product with the 30-mer substrate (product/substrate). The data are expressed as machine counts/μg of protein.

ROPS

The relative number of 3′-OH group-containing DNA strand breaks was quantified using a Klenow(exo$^-$) incorporation assay based on the ability of Klenow to initiate DNA synthesis from a 3′-OH (31). DNA was heat-denatured at 100 °C for 5 min, and 0.25 μg of DNA was added to 15 μl of a Klenow reaction buffer (0.5 mM dTTP, 0.5 mM dGTP, 0.5 mM dATP, 0.33 μM dCTP, 5 units of Klenow(exo$^-$) (New England Biolabs, Beverly, MA)) with 10× Klenow buffer per the manufacturer's protocol (New England Biolabs) and 5 μCi of [α-^{32}P]dCTP (3000 Ci/mmol; PerkinElmer Life Sciences). Reaction mixtures were incubated at 16 °C for 30 min, and the reaction was stopped with the addition of 25 μl of 12.5 mM EDTA, pH 8.0. Samples were spotted (5 μl) onto scored and numbered Whatman DE81 chromatography paper and allowed to air-dry. The chromatography paper was then washed five times for 5 min each time in 0.5 M Na_2HPO_4 (dibasic) to remove unincorporated [α-^{32}P]dCTP and then rinsed twice briefly in water and allowed to air-dry. Paper was cut and placed into scintillation vials with 2.5 ml of Scinti Verse mixture (Fisher). Incorporation of [α-^{32}P]dCTP was quantified using a Packard scintillation counter.

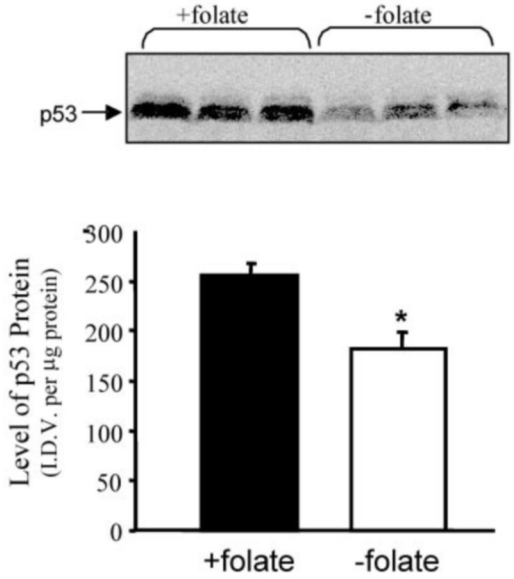

FIG. 3. **Analysis of p53 protein levels in liver of mice fed a folate-deficient or -adequate diet.** Samples of images of Western blots of p53 protein levels in liver of mice fed the purified isoenergetic diets containing either 2 mg/kg folic acid (folate-adequate) or 0 mg/kg folic acid (folate-deficient) are shown. Crude nuclear extracts were isolated from liver tissues of mice, and the levels of p53 protein in 50 μg of nuclear extract were determined by Western blot analysis using an ECL detection kit. The relative level of p53 protein was determined by Western blot analysis using antisera developed against mouse p53. The bands were detected and quantified using an AlphaInnotech ChemiImager™ system. The data are expressed as the I.D.V. of the band/μg of protein loaded. Values are expressed as mean ± S.E. for data obtained from at least 10 animals in each group. *, value significantly different from mice fed the folate-supplemented diet at $p < 0.01$. *Filled bar*, 2 mg/kg folic acid; *open bar*, 0 mg/kg folic acid.

Statistical Analysis

Statistical significance between means was determined using analysis of variance followed by Fisher's least significant difference test where appropriate (32). A p value less than 0.05 was considered statistically significant.

RESULTS

In an extensive study, we have carefully characterized the effect of folate deficiency on weight gain/loss and plasma folate levels in C57BL/6 mice. Throughout the 8-week feeding study, the animals' food intake and body weights were monitored twice weekly. Long term folate deficiency can result in toxicity, evidenced primarily by weight loss. Importantly, in our studies, no difference in food intake or weight gain/loss was observed (Fig. 1*A*). It is essential to demonstrate that the experimental diet (0 mg/kg folic acid) resulted in decreased serum folate levels. As expected, a significant decrease in the level of serum folate in the folate-deficient mouse was observed. The 0 mg/kg folic acid group had serum folate levels 93% lower than the control animals ($p < 0.001$), such that the folate levels of the deficient animals approached zero (Fig. 1*B*). The addition of 1% succinyl sulfathiazole allowed attainment of this severity of folate deficiency by preventing intestinal production of folates. Since vitamin B_{12} can alter one-carbon metabolism through its participation in the methionine synthase reaction, it was important to determine whether our results might be confounded by changes in serum B_{12} levels. Importantly, no differences were observed in B_{12} levels between control and deficient groups (data not shown). There was no effect of β-pol heterozygosity on weight or serum folate levels in response to folate deficiency (data not shown).

This is the first investigation to directly measure the effect of folate deficiency on BER capacity. It is the BER pathway that

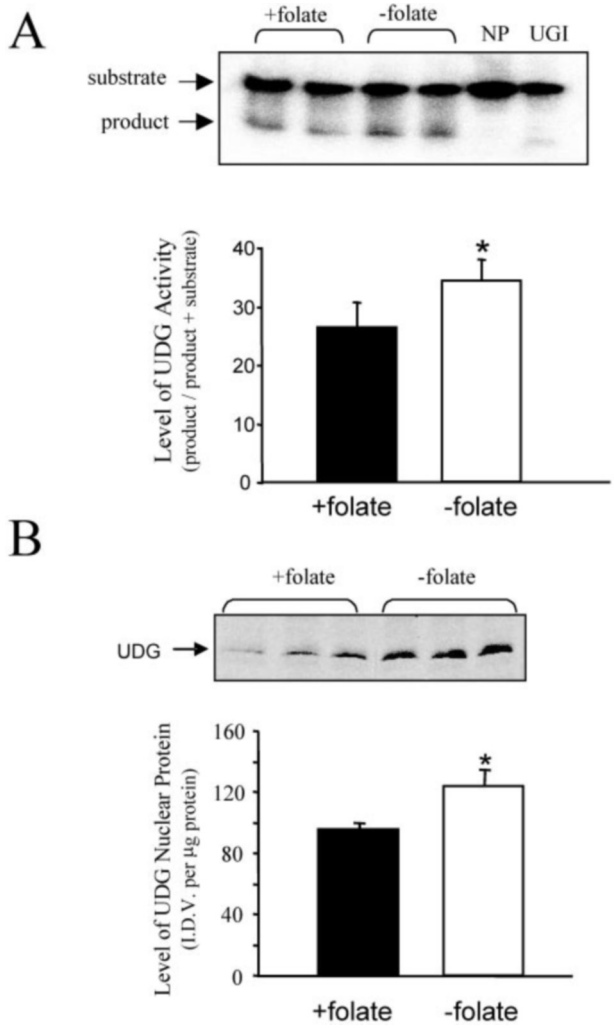

FIG. 4. **Analysis of UDG activity and protein levels in liver of mice fed a folate-deficient or -adequate diet.** The experiments were conducted using crude nuclear extracts as described under "Experimental Procedures." *A*, an autoradiograph of a sequencing gel indicating UDG enzymatic activity as visualized by the appearance of a 12-base fragment. The ability of UDG to excise uracil was analyzed using a ^{32}P-end-labeled 30-mer single strand uracil-containing DNA substrate (2.5 pmol) incubated with 5 μg of crude nuclear extract from liver of mice fed the folate-adequate or folate-deficient diets. UDG activity (presence of an 11-base fragment) was visualized and quantified using a Molecular Imager® System by calculating the relative amount of the 11-base product with the 30-base substrate (product/(product + substrate)). The data are expressed as machine counts/μg of protein. All values represent an average ± S.E. for data obtained from at least 10 animals in each group. *N*, negative control, reaction contained no protein; *UGI*, the addition of UDG inhibitor to reaction; *, value significantly different from mice fed the folate supplemented diet at $p < 0.05$. *B*, samples of *images* of Western blots of UDG protein levels in liver of mice fed the folate-adequate or folate-deficient diets are shown. The relative level of the UDG protein was determined by Western blot analysis using antiserum developed against mouse UDG. The bands were detected and quantified using an AlphaInnotech ChemiImager™ system. The data are expressed as the I.D.V. of the band/μg of protein loaded. Values are expressed as mean ± S.E. for data obtained from at least 10 animals in each group. *, value significantly different from mice fed the folate-supplemented diet at $p < 0.01$. *Filled bar*, 2 mg/kg folic acid; *open bar*, 0 mg/kg folic acid.

holds primary responsibility for removing folate-induced damage from DNA. Previously we (24) and others (23, 33, 34) have shown BER to be DNA damage-inducible. As such, we should expect BER to be up-regulated in response to the increased levels of DNA damage that occur in folate deficiency. Surprisingly, we observed no increase in BER activity in response to folate deficiency (Fig. 2*A*). Additionally, it has been clearly

determined that β-pol levels are rate-determining in BER (16). In agreement, we show that the lack of inducibility of BER in response to folate deficiency is preceded by a lack of induction in β-pol (Fig. 2*B*). Again, this is surprising, since we expected to see an induction in β-pol in response to the stress of folate deficiency.

In culture, folate deficiency has been shown to increase p53 levels (35, 36) and arrest cells in S-phase (37, 38), ostensibly as a result of the imbalance in nucleotide precursors that occurs when folate is limiting. In contrast, in response to folate deficiency *in vivo*, we observe a 20% reduction in nuclear p53 levels (Fig. 3, $p < 0.01$). Whereas this contradicts cell culture data, it is in agreement with gene profiling data from Crott *et al.* (39), who demonstrate a reduction in p53 transcription in colonic mucosa from adult animals in response to folate deficiency. Although BER can proceed in the absence of p53, a role for p53 in regulating BER has been described (40, 41). Whether the observed decline in p53 in response to folate deficiency is related to the inability to induce BER remains to be determined.

The lack of induction in BER activity in response to folate deficiency supports the hypothesis that folate deficiency results in an inability to repair DNA damage. It is important to make a distinction between BER activity and activity of enzymes within this pathway. Individual enzymes within the pathway may be altered without changing the overall balance of the entire pathway and could potentially explain the accumulation of intermediate DNA repair products. To investigate whether imbalance within BER occurs in response to folate deficiency, we assessed the protein levels and enzyme activities of key proteins within this pathway. As discussed above, it is clear that folate deficiency does not up-regulate the ability to completely repair DNA damage, an effect exerted at the level of β-pol expression. This lack of BER induction in response to folate deficiency has caused us to evaluate this question with respect to uracil removal.

Synthesis of thymidylate is altered in response to folate deficiency, resulting in an accumulation of dUMP in nucleotide pools (6). As a result, uracil becomes misincorporated into DNA. In response, a specific and efficient enzyme, UDG, catalyzes the removal of uracil from DNA. This represents the first step in the BER pathway for removal of uracil. In response to folate deficiency, we observed a 31% increase in UDG activity (Fig. 4*A*, $p < 0.05$). This corresponds to a 30% increase in nuclear UDG protein levels in response to folate deficiency (Fig. 4*B*, $p < 0.01$). The increased UDG response to folate deficiency without a subsequent increase in BER and β-pol represents a dysregulation in coordination of BER that could result in the detrimental accumulation of genotoxic DNA repair intermediates.

Following UDG-initiated removal of uracil, a transient abasic site was created. This site was cut by an endonuclease to generate the 3′-OH required for repair synthesis. The endonuclease responsible for this incision of the DNA is believed to be Ape. In response to folate deficiency, we observed no effect on either Ape protein levels (Fig. 5*A*) or Ape endonuclease activity (Fig. 5*B*). It is presently unclear whether the lack of induction in Ape protein and activity is physiologically relevant. Both protein levels and enzymatic activity have been shown to be DNA damage-inducible (42). However, Ape is not rate-limiting in BER and may even be dispensable for BER (43). As such, the impact that its lack of induction will have is questionable.

As discussed above, the removal of uracil by UDG creates a transient abasic site that must be further processed in order for repair synthesis to occur. When repair is initiated but not completed, intermediate repair products can be expected to accumulate. The type of intermediate that accumulates can indicate where BER has stalled. Since neither Ape nor β-pol is induced in response to folate deficiency, we might expect to see an accumulation of abasic sites, an accumulation of single

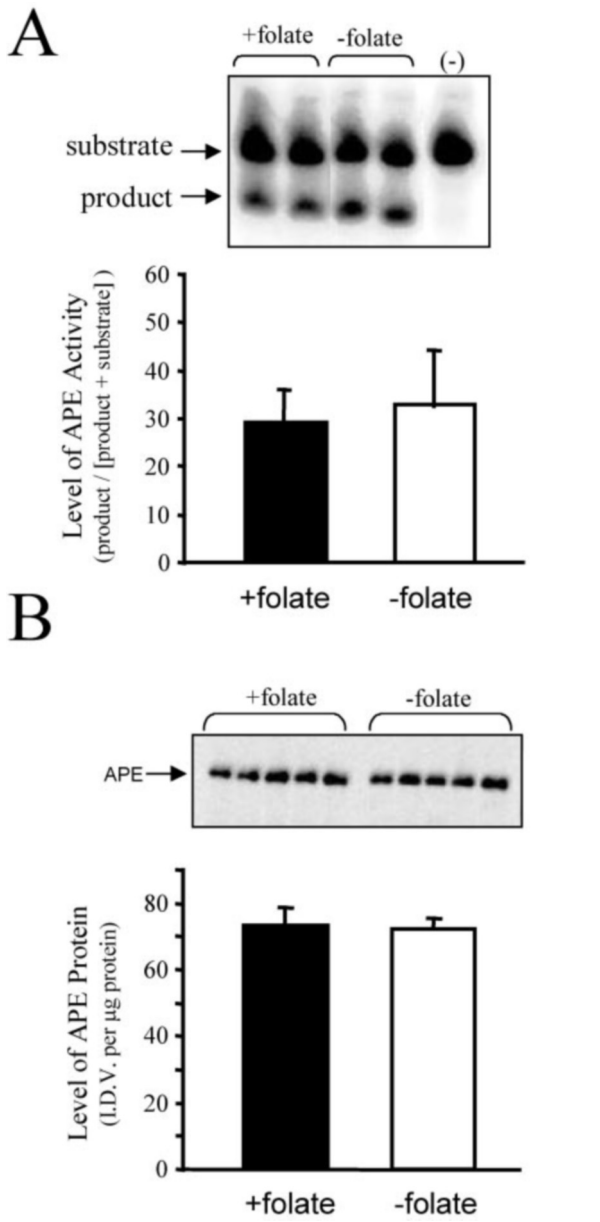

FIG. 5. **Effect of dietary folate on Ape enzymatic activity and Ape protein levels.** The experiments were conducted using crude nuclear extracts as described under "Experimental Procedures." *A*, an autoradiograph of a sequencing gel indicating Ape endonuclease activity as visualized by the appearance of a 14-base fragment. The 5′-endonuclease activity of Ape was analyzed using a ^{32}P-end-labeled 26-mer duplex AP-DNA substrate (2.5 pmol) incubated with 100 ng of crude nuclear extract from liver of mice fed the folate-adequate or folate-deficient diets. Endonuclease activity (presence of a 14-base fragment) was visualized and quantified using a Molecular Imager® system by calculating the relative amount of the 14-base product with the unreacted 26-base substrate (product/(product + substrate)). The data are expressed as machine counts/ng of protein. All values represent an average ± S.E. for data obtained from at least 10 animals in each group. *B*, samples of *images* of Western blots of Ape protein levels in liver of mice fed the folate-adequate or folate-deficient diets are shown. The relative level of the 37-kDa Ape protein was determined by Western blot analysis using monoclonal antisera developed against mouse Ape. The bands were detected and quantified using an AlphaInnotech ChemiImager™ system. The data are expressed as the I.D.V. of the band per μg of protein loaded. Values are expressed as mean ± S.E. for data obtained from at least 10 animals in each group. *Filled bar*, 2 mg/kg folic acid; *open bar*, 0 mg/kg folic acid.

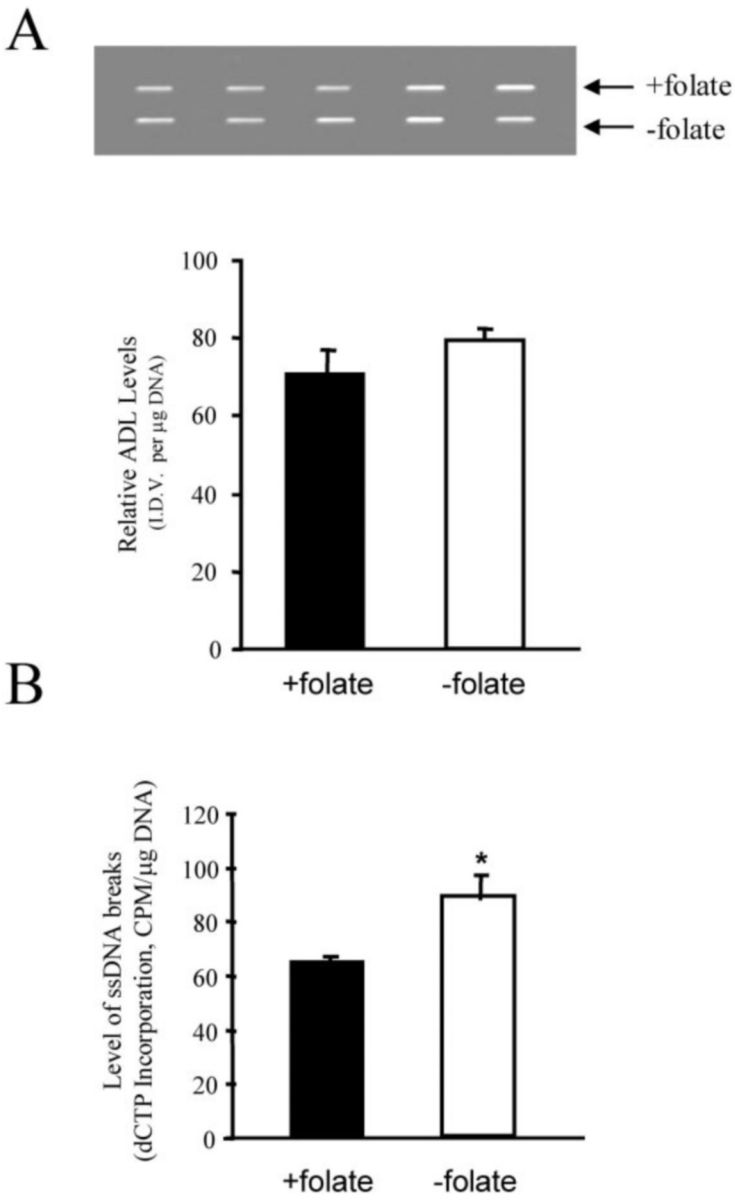

FIG. 6. **Analysis of DNA repair intermediates in liver DNA of mice fed a folate-deficient or -adequate diet.** *A*, liver DNA was isolated from liver tissue of mice fed the folate-deficient and folate-adequate diets using the TEMPO extraction methodology, and the levels of ADLs were measured using the ASB assay as described under "Experimental Procedures." The data are expressed as the I.D.V. of the band/μg of DNA loaded. Values represent an average ± S.E. for data obtained from at least 10 animals in each group. *B*, liver DNA was isolated using gravity tip extraction columns, and the number of single strand (*ssDNA*) breaks was measured using the ROPS assay as described under "Experimental Procedures." The data are expressed as machine counts/min (*CPM*)/μg of DNA corresponding to the level of [α-^{32}P]dCTP incorporation as quantified by a Packard scintillation counter. Values represent an average ± S.E. for data obtained from at least 10 animals in each group. *, value significantly different from mice fed the folate-supplemented diet at $p < 0.01$. *Filled bar*, 2 mg/kg folic acid; *open bar*, 0 mg/kg folic acid.

strand breaks, or a combination of both. In response to folate deficiency, we observe no increase in the level of abasic sites (Fig. 6*A*). The lack of accumulation of abasic sites demonstrates that Ape activity is adequate to process the abasic site and, in the process, generate a single strand break.

Single strand breaks have been previously shown to accumulate in response to folate deficiency (9, 10, 15, 18, 19). We have verified that our folate-deficient feeding has likewise resulted in the accumulation of single strand breaks using the ROPS assay developed by the James laboratory (31). In response to folate deficiency, we observed a 37% increase in the level of single strand breaks (Fig. 6*B*, $p < 0.05$). In BER, the strand break created during repair persists until the rate-limiting step performed by β-pol is completed, at which point ligation can occur. We suggest that these strand breaks arise as a function of efficient removal of uracil and persist due to inadequate β-pol activity.

In support of this mechanism of strand break accumulation, we observed an even greater increase in strand breaks in β-pol-haploinsufficient mice that are folate-deficient. In wild type mice, folate deficiency induced a 37% increase in DNA strand breaks (Fig. 6*B*), and this increased to 52% in the β-pol-haploinsufficient mice (Fig. 7). However, no significant increase in ADLs was observed in wild type mice in response to folate deficiency, whereas a 38% increase was observed (Fig. 8; $p < 0.01$) in the β-pol-haploinsufficient mice. This is the first experimental observation of an increased level of ADLs *in vivo* and demonstrates that haploinsufficiency in β-pol reduces the efficiency by which these lesions are processed.

DISCUSSION

This study represents the first direct investigation into the effect of folate deficiency on the capacity of the BER pathway. As discussed, experimental evidence strongly suggests a reduced ability to repair DNA damage induced by folate deficiency. We demonstrate here that when folate is deficient, BER is unable to mount an adequate response to process the DNA damage induced by folate deficiency. This is surprising, since BER is clearly a DNA damage-inducible pathway (23, 24, 33, 34). Folate deficiency results in nucleotide depletion (6, 44), and we suggest that this depletion may be affecting the inducibility of β-pol. Clearly, DNA polymerases require that deoxyribonucleotides exist in proper balance for optimal functioning. This inability to induce β-pol causes a phenotype of reduced BER efficiency. This functional BER deficiency ultimately

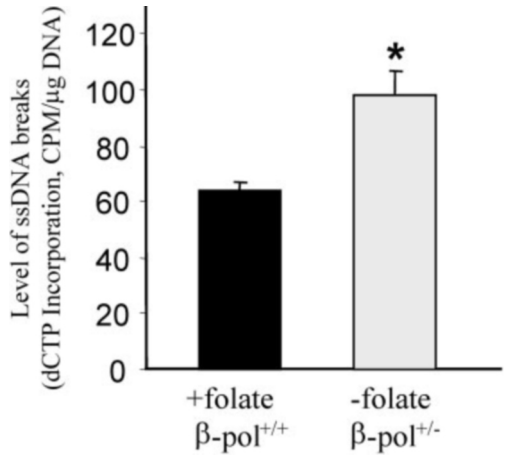

FIG. 7. **Analysis of DNA single strand breaks in liver DNA of β-pol$^{+/+}$ mice fed a folate-adequate diet and β-pol$^{+/-}$ mice fed a folate-deficient diet.** Liver DNA was isolated using gravity tip extraction columns, and the number of single strand (*ssDNA*) breaks was measured using the ROPS assay as described under "Experimental Procedures." The data are expressed as machine counts/min (*CPM*)/μg of DNA, corresponding to the level of [α-^{32}P]dCTP incorporation as quantified by a Packard scintillation counter. Values represent an average ± S.E. for data obtained from at least 10 animals in each group. *, value significantly different from mice fed the folate-supplemented diet at $p < 0.01$. *Filled bar*, β-pol$^{+/+}$ mice fed 2 mg/kg folic acid; *open bar*, β-pol$^{+/-}$ mice fed 0 mg/kg folic acid.

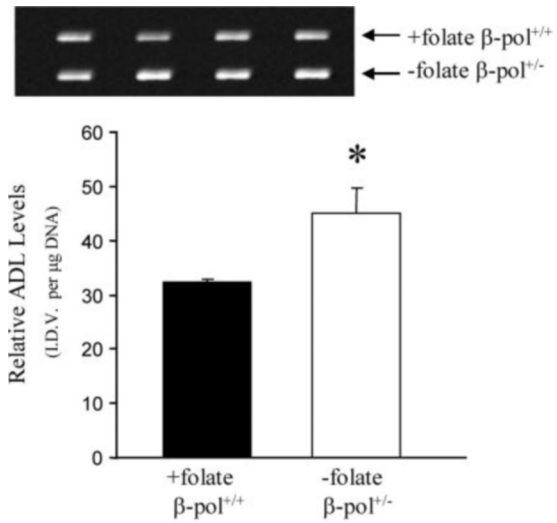

FIG. 8. **Analysis of aldehydic DNA lesions in liver DNA of β-pol$^{+/+}$ mice fed a folate-adequate diet and β-pol$^{+/-}$ mice fed a folate-deficient diet.** Liver DNA was isolated from liver tissue of mice fed the folate-deficient and folate-adequate diets using the TEMPO extraction methodology, and the levels of ADLs were measured using the ASB assay as described under "Experimental Procedures." The data are expressed as the I.D.V. of the band/μg of DNA loaded. Values represent an average ± S.E. for data obtained from at least 10 animals in each group. *, value significantly different from mice fed the folate-supplemented diet at $p < 0.01$. *Filled bar*, β-pol$^{+/+}$ mice fed 2 mg/kg folic acid; *open bar*, β-pol$^{+/-}$ mice fed 0 mg/kg folic acid.

causes an accumulation of toxic DNA repair intermediates that is exacerbated by β-pol haploinsufficiency.

Folate deficiency alters the balance and coordination of BER by stimulating initiation of BER without subsequently stimulating the rate-limiting step in the repair process. Inducibility of UDG has been previously demonstrated (45, 46), but this is the first report of UDG induction in response to folate deficiency or any dietary manipulation. Additionally, we demonstrate a tight correlation between levels of UDG protein and UDG activity, suggesting that UDG activity is regulated by levels of UDG protein. The abasic sites generated by accelerated UDG activity are rapidly processed in wild type animals, as evidenced by our inability to detect an increased level of abasic sites in response to folate deficiency. However, this rapid processing of abasic sites is not due to increased levels of Ape protein or Ape activity, since we observe no effect of folate deficiency on this enzyme. This is in contrast to data from Courtemanche *et al.* (38), who show up-regulation in Apex/Ape mRNA in response to *in vitro* folate deprivation. Perhaps differences between an *in vivo* system and a cell culture system exist, or perhaps the inducibility of Ape observed by Courtemanche *et al.* (38) is a response to increased redox requirements, which may shuttle Ape to the cytoplasm. We do not believe that an inability to increase Ape activity in response to folate deficiency is an important biological mechanism in the processing of abasic sites, since we have previously demonstrated that one-half the gene dosage of Ape does not result in an accumulation of abasic sites (47).

On the other hand, the highly efficient processing of abasic sites results in an accumulation of substrate for the rate-determining enzyme in BER, β-pol. As a combined result of increased substrate for β-pol and lack of induction in β-pol, repair stalls and single strand breaks accumulate. We verify that folate deficiency results in an accumulation of strand breaks and that these breaks are specifically 3′-OH-containing lesions. Having previously shown that β-pol is directly responsible for the accumulation of strand breaks in response to oxidative damage (24), the lack of an adequate β-pol response is the likely explanation for the accumulation of strand breaks when folate is deficient. Strongly in support of the role for β-pol in preventing the resolution of these strand breaks is the increased accumulation of repair intermediates in response to folate deficiency when β-pol is haploinsufficient.

To address whether an underlying BER deficiency would exacerbate the effects of folate deficiency, we subjected β-pol-haploinsufficient mice to folate deficiency. The lack of inducibility of β-pol and BER in response to folate deficiency in combination with a 50% reduced BER capacity results in an increased accumulation of DNA strand breaks as well as an increase in ADLs. This is the first *in vivo* demonstration of an increased persistence of these aldehydic groups and requires some discussion. These ADLs could represent intact abasic sites resulting from base removal in the absence of subsequent endonuclease activity. However, this seems unlikely, since Ape1 activity is neither rate-determining nor affected by folate deficiency. Furthermore, abasic sites are very efficiently processed, making their detection nearly impossible. We propose a mechanism whereby deficiency in β-pol causes both strand breaks and aldehydic lesions to accumulate as part of the same lesion, directly as a result of β-pol insufficiency. The proposed mechanism is consistent with previous observations that repair of abasic sites is 7-fold faster than repair of uracil, which is 4-fold faster than the repair of 8OHdG (48).

In the haploinsufficient mouse, both 3′-OH groups and free aldehyde groups accumulate. Fig. 9*A* demonstrates how the removal of uracil by UDG creates a transient intact abasic site that is processed by Ape1 such that both an aldehyde group detectable by the aldehyde reactive probe and a 3′-OH group detectable by Klenow incorporation are present. We suggest that in the β-pol-haploinsufficient mouse, this 3′-OH/aldehydic lesion persists, directly as a result of the reduced ability to insert a new nucleotide, excise the deoxyribose flap, and complete repair. In a model with adequate levels of β-pol, this 3′-OH/aldehydic lesion should not persist, and in fact, it does not. The wild type mice subjected to folate deficiency accumulate only the 3′-OH lesions in the absence of the aldehydic lesions. Our hypothesis that folate deficiency exerts its effects

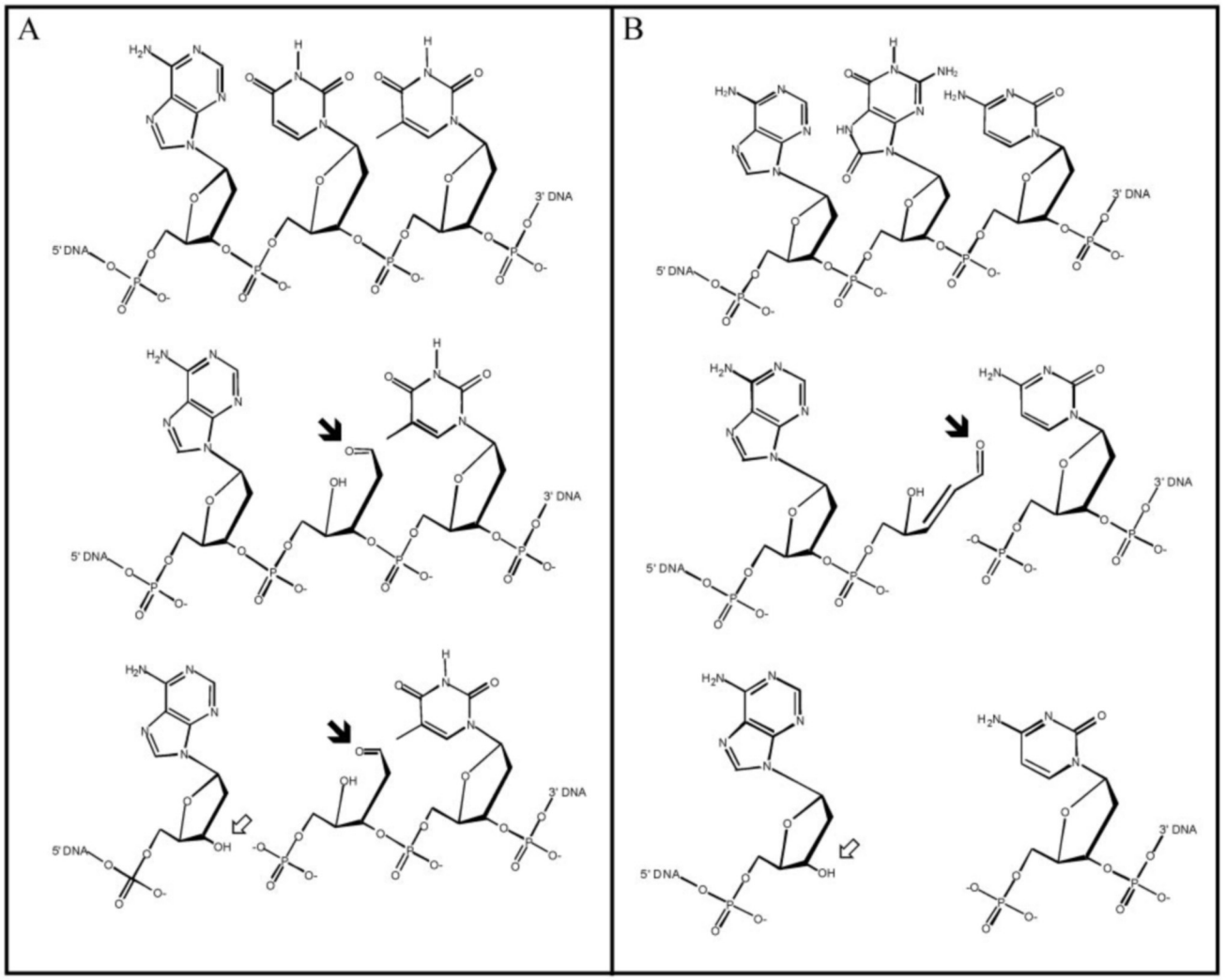

FIG. 9. **Processing of uracil and 8OHdG lesions by monofunctional UDG (*A*) and bifunctional DNA glycosylase (*OGG1*) (*B*) and Ape is shown.** The *solid arrows* and *open arrow* point to aldehydic DNA lesions and DNA 3′-OH, respectively.

by altering regulation of β-pol seems faulty if different classes of lesions arise in the β-pol model as compared with the wild type model in response to folate deficiency. This is addressed in Fig. 9*B*, which depicts the mechanism by which 3′-OH groups can accumulate without a corresponding accumulation in aldehyde groups. In this case, the first step of repair involves removal of the damaged base by a bifunctional glycosylase, generating a strand break that does not contain a 3′-OH group but does contain an aldehyde group. This is not a lesion we have been able to detect. The second step is the trimming of the 3′-phosphoglycolate, which removes the aldehyde group and generates a 3′-OH group. This is consistent with the lesions we have been able to detect in response to folate deficiency in wild type animals. These data support previous data (48) demonstrating a preference for the repair of abasic sites and uracil over the repair of oxidized bases, like 8OHdG. Oxidized bases can be expected to arise both as a result of cellular metabolism and as a result of increased homocysteine levels in response to folate deficiency. As such, we propose that in wild type animals both uracil and oxidized bases are being processed, but shuttling toward repair of uracil prevents the accumulation of uracil-initiated repair intermediates while forcing the accumulation of repair intermediates arising from bifunctional glycosylases. However, in the face of β-pol haploinsufficiency, β-pol levels fall to a critically low level such that all of the repair intermediates begin to accumulate.

When the amount of β-pol is limiting, as it is in the β-pol-haploinsufficient mouse and as we now know it is in folate deficiency, BER is thrown out of balance, and toxic repair intermediates accumulate. This accumulation of repair intermediates is critically dependent on glycosylase-mediated removal of the damaged base, and we suggest that the up-regulation in UDG activity is a critical factor in the phenotype resulting from folate deficiency. This is supported by the ability of an *UNG1* deletion to rescue *apn1/apn2/rad1* lethality (49).

The inability of folate deficiency to induce BER results in a functional BER deficiency. Having previously established that BER deficiency in the β-pol-haploinsufficient mouse predisposes to cancer, we suggest that the functional BER deficiency induced by folate deficiency will likewise predispose to cancer, primarily by reducing DNA damage tolerance. We have clearly shown that reduced BER capacity in response to β-pol haploinsufficiency (17) and in response to aging (50) reduces the threshold of DNA damage tolerance. Folate deficiency likewise reduces tolerance to DNA damage (7–11), further support that BER deficiency is responsible for the phenotype expressed by folate deficiency. Additionally, a genetic defect in β-pol intensifies the effects of folate deficiency, demonstrating that β-pol haploinsufficiency and folate deficiency interact to increase cancer risk. Future investigations should focus on identifying important cis-acting (*e.g.* promoter methylation) and trans-acting factors important in regulating β-pol in response to

folate deficiency. Presently, these data provide evidence that gene/nutrient as well as nutrient/environment interactions exist that predispose to cancer and that in both cases regulation of DNA polymerase β is a critical factor.

Acknowledgments—We thank Drs. Samuel H. Wilson (NIEHS) and Robert W. Sobol (University of Pittsburgh Cancer Institute) for the generous gift of the DNA polymerase $\beta^{+/-}$ mice. We also thank Dr. Ashok S. Bhagwat and Michael Carpenter (Wayne State University) for invaluable discussions pertaining to the chemical nature of base excision repair intermediates.

REFERENCES

1. Glynn, S. A., and Albanes, D. (1994) *Nutr. Cancer* **22,** 101–119
2. Choi, S. W., and Mason, J. B. (2000) *J. Nutr.* **130,** 129–132
3. Cravo, M. L., Mason, J. B., Dayal, Y., Hutchinson, M., Smith, D., Selhub, J., and Rosenberg, I. H. (1992) *Cancer Res.* **52,** 5002–5006
4. Kim, Y. I., Salomon, R. N., Graeme-Cook, F., Choi, S. W., Smith, D. E., Dallal, G. E., and Mason, J. B. (1996) *Gut* **39,** 732–740
5. Hoover, K. L., Lynch, P. H., and Poirier, L. A. (1984) *J. Natl. Cancer Inst.* **73,** 1327–1336
6. James, S. J., Miller, B. J., Basnakian, A. G., Pogribny, I. P., Pogribna, M., and Muskhelishvili, L. (1997) *Carcinogenesis* **18,** 287–293
7. Branda, R. F., Hacker, M., Lafayette, A., Nigels, E., Sullivan, L., Nicklas, J. A., and O'Neill, J. P. (1998) *Environ. Mol. Mutagen.* **32,** 33–38
8. Branda, R. F., Lafayette, A. R., O'Neill, J. P., and Nicklas, J. A. (1999) *Mutation Res.* **427,** 79–87
9. Duthie, S. J., and Hawdon, A. (1998) *FASEB J.* **12,** 1491–1497
10. Duthie, S. J., Narayanan, S., Blum, S., Pirie, L., and Brand, G. M. (2000) *Nutr. Cancer* **37,** 245–251
11. Kruman, I. I., Kumaravel, T. S., Lohani, A., Pedersen, W. A., Cutler, R. G., Druman, Y., Haughey, N., Lee, J., Evans, M., and Mattson, M. P. (2002) *J. Neurosci.* **22,** 1752–1762
12. Choi, S. W., Kim, Y. I., Weitzel, J. N., and Mason, J. B. (1998) *Gut* **4***,* 93–99
13. Wickramasinghe, S. N., and Fida, S. (1994) *Blood* **83,** 1656–1661
14. Blount, B. C., Mack, M. M., Wehr, C. M., MacGregor, J. T., Hiatt, R. A., Wang, G., Wickramasinghe, S. N., Everson, R. B., and Ames, B. N. (1997) *Proc. Natl. Acad. Sci. U. S. A.* **94,** 3290–3295
15. Duthie, S. J., Grant, G., and Narayanan, S. (2000) *Br. J. Cancer* **83,** 1532–1537
16. Srivastava, D. K., Vande Berg, B. J., Prasad, R., Molina, J. T., Beard, W. A., Tomkinson, A. E., and Wilson, S. H. (1998) *J. Biol. Chem.* **273,** 21203–21209
17. Cabelof, D. C., Guo, Z., Raffoul, J. J., Sobol, R. W., Wilson, S. H., Richardson, A., and Heydari, A. R. (2003) *Cancer Res.* **63,** 5799–5807
18. Melnyk, S., Pogribna, M., Miller, B. J., Basnakian, A. G., Pogribny, I. P., and James, S. J. (1999) *Cancer Lett.* **146,** 35–44
19. Kim, Y. I., Shirwadkar, S., Choi, S. W., Puchyr, M., Wang, Y., and Mason, J. B. (2000) *Gastroenterology* **119,** 151–161
20. Branda, R. F., Lafayette, A. R., O'Neill, J. P., and Nicklas, J. A. (1997) *Cancer Res.* **57,** 2586–2588
21. MacGregor, J. T., Schlegel, R., Wehr, C. M. Alperin, P., and Ames, B. N. (1990) *Proc. Natl. Acad. Sci. U. S. A.* **87,** 9962–9965
22. Everson, R. B., Wehr, C. M., Erexson, G. L., and MacGregor, J. T. (1988) *J. Natl. Cancer Inst.* **80,** 525–529
23. Fornace, A. J., Jr., Zmudzka, B., Hollander, M. C., and Wilson, S. H. (1989) *Mol. Cell. Biol.* **9,** 851–853
24. Cabelof, D. C., Raffoul, J. J., Yanamadala, S., Guo, Z., and Heydari, A. R. (2002) *Carcinogenesis* **23,** 1419–1425
25. Horton, J. K., Joyce-Gray, D. F., Pachkowski, B. F., Swenberg, J. A., and Wilson, S. H. (2003) *DNA Repair* **2,** 27–48
26. Gu, H., Marth, J. D., Orban, P. C., Mossmann, H., and Rajewsky, K. (1994) *Science* **265,** 103–106
27. Hofer, T., and Moller, L. (1998) *Chem. Res. Toxicol.* **11,** 882–887
28. Nakamura, J., Walker, V. E., Upton, P. B., Chiang, S. Y., Kow, Y. W., and Swenberg, J. A. (1998) *Cancer Res.* **58,** 222–225
29. Stuart, J. A., Karahalil, B., Hogue, B. A., Souza-Pinto, N. C., Bohr, V. A. (2004) *FASEB J.* **18,** 595–597
30. Wilson, D. M., III, Takeshita, M., Grollman, A. P., and Demple, B. (1995) *J. Biol. Chem.* **270,** 16002–16007
31. Basnakian, A. G., and James, S. J. (1996) *DNA Cell Biol.* **15***,* 255–262
32. Sokal, R. R., and Rohlf, F. J. (1981) *Biometry*, pp. 169–176, W.H. Freeman and Co., New York
33. Chen, K. H., Yakes, F. M., Srivastava, D. K., Singhal, R. K., Sobol, R. W., Horton, J. K., vanHouten, B., and Wilson, S. H. (1998) *Nucleic Acids Res.* **26,** 2001–2007
34. Lin, L. H., Cao, S., Yu, L., Cui, J., Hamilton, W. J., and Liu, P. K. (2000) *J. Neurochem.* **74,** 1098–1105
35. Bronder, J. L., and Moran, R. G. (2003) *J. Biol. Chem.* **278,** 48861–48871
36. Linke, S. P., Clarkin, K. C., DiLeonardo, A., Tsou, A., and Wahl, G. M. (1996) *Genes Dev.* **10,** 934–947
37. Koury, M. J., Price, J. O., and Hicks, G. G. (2000) *Blood* **96,** 3249–3255
38. Courtemanche, C., Huang, A. C., Elson-Schwab, I., Kerry, N., Ng, B. Y., and Ames, B. N. (2004) *FASEB J.* **18,** 209–211
39. Crott, J. W., Choi, S. W., Ordovas, J. M., Ditelberg, J. S., and Mason, J. B. (2004) *Carcinogenesis* **25,** 69–76
40. Zhou, J., Ahn, J., Wilson, S. H., and Prives, C. (2001) *EMBO J.* **20,** 914–923
41. Offer, H., Milyavsky, M., Erez, N., Matas, D., Zurer, I., Harris, C. C., and Rotter, V. (2001) *Oncogene* **20,** 581–589
42. Fritz, G., Grosch, S., Tomicic, M., and Kaina, B. (2003) *Toxicology* **193,** 67–78
43. Izumi, T., Wiederhold, L. R., Roy, G., Roy, R., Jaiswal, A., Bhakat, K. K., Mitra, S., and Hazra, T. K. (2003) *Toxicology* **193,** 43–65
44. Walzem, R. L., Clifford, C. K., and Clifford, A. J. (1983) *J. Nutr.* **113,** 1032–1038
45. Sirover, M. A. (1979) *Cancer Res.* **39,** 2090–2095
46. Williams, M. V., Winters, T., and Waddell, K. S. (1987) *Mol. Pharmacol.* **31,** 200–207
47. Raffoul, J. J., Cabelof, D. C., Nakamura, J., Meira, L. B., Friedberg, E. C., and Heydari, A. R. (2004) *J. Biol. Chem.* **279,** 18425–18433
48. Cappelli, E., Hazra, T., Hill, J. W., Slupphaug, G., Bogliolo, M., and Frosina, G. (2001) *Carcinogenesis* **22,** 387–393
49. Guillet, M., and Boiteux, S. (2003) *Mol. Cell. Biol.* **23,** 8386–8394
50. Cabelof, D. C., Raffoul, J. J., Yanamadala, S., Ganir, C., Guo, Z., and Heydari, A. R. (2003) *Mutat. Res.* **500,** 135–145